

A FUNDAMENTAL SEQUENCES METHOD FOR AN INVERSE BOUNDARY VALUE PROBLEM FOR THE HEAT EQUATION IN DOUBLE-CONNECTED DOMAINS

IHOR BORACHOK✉*¹ AND ROMAN CHAPKO✉¹

¹Faculty of Applied Mathematics and Informatics,
Ivan Franko National University of Lviv, Ukraine

(Communicated by Elena Beretta)

ABSTRACT. The application of the fundamental sequences method for reconstructing the inner part of the boundary of a double-connected domain from the overdetermined Cauchy data of the solution of the heat conduction equation on the outer part of the boundary is considered. The nonlinear ill-posed problem is numerically solved by the regularized Newton's method, at each step of which direct problems for the heat equation are solved. Using Rothe's method, each direct problem is reduced to a sequence of elliptic Dirichlet problems for the inhomogeneous modified Helmholtz equation. Which, in turn, is fully discretized by the fundamental sequences method. The results of numerical examples in both two- and three-dimensional domains confirm the accuracy of the proposed method with negligible computational effort.

1. Introduction. The problem of reconstruction of the shape of the zero-temperature inclusion inside a solid or liquid body from measurements of temperature and heat flux on the outer boundary is described by the considered nonlinear inverse boundary value problem for the heat conduction equation. In [10], regularized Newton's iterative method is proposed, at each step, a linearized equation is constructed by solving direct problems for the heat equation. The boundary integral equations method is proposed for solving direct problems, which shows a good result, but requires difficult calculations and expensive computational costs, see also [6, 14]. A more practical problem is considered in [11], when the heat flux is zero at the unknown inner boundary, again, the corresponding direct problems are solved using the integral equations approach. Both problems are considered for two-dimensional domains.

Three-dimensional domains case is a less studied. There are already several works, but regarding steady state inverse problems [7, 15], through a complex numerical algorithm for solving three-dimensional linear problems by the boundary integral equations method, see [5]. In our work, we propose a numerical method that can be applied to two- and three-dimensional domains without much computational effort.

2020 *Mathematics Subject Classification.* Primary: 35K05, 65N80, 49M15, 47J06; Secondary: 80M20, 65M30.

Key words and phrases. Boundary reconstruction problem, heat equation, Rothe's method, fundamental sequences method, Tikhonov regularization, Newton's method.

*Corresponding author: Ihor Borachok.

The proposed method is built on the iterative procedure developed in [10] and the two-step numerical method for solving the direct problem [4]. As in [10], the inverse problem is represented in the form of a nonlinear equation, which is solved by Newton's method. The results of the nonlinear mapping and its domain derivative are described as normal derivatives of solutions of forward time dependent problems. Next, each direct problem is reduced to a sequence of stationary problems, using Rothe's method. Finally, the sequence of stationary problems is fully discretized by the fundamental sequences method.

The fundamental sequences method [3, 4] is built on the method of fundamental solutions [12, 17], but for the case of the sequence of stationary problems with inhomogeneous equations. The unknown functions are approximated by linear combinations of elements of the fundamental sequence that exactly satisfy the governing equation. The unknown coefficients in the approximations are found by collocation on the boundaries, matching the boundary conditions.

The linearized equation, obtained at each step of Newton's method, is solved by the collocation method, and its solution is approximated by a linear combination of elements from the corresponding finite-dimensional subspace.

Here we note that the classical method of fundamental solutions has been successfully used for the boundary reconstruction in the stationary case, see [16, 20]. Our contribution is to extend its advantages to the non-stationary case.

Let's describe the problem to be studied in more detail. The solution domain D is a double-connected domain in \mathbb{R}^d , $d = 2, 3$, with the inner boundary Γ_1 and the outer boundary Γ_2 . Each part of the domain's boundary is a simple closed curve (or surface for $d = 3$) of class C^2 , and the two parts do not intersect. First, we consider the following direct initial boundary value problem for the heat equation

$$\begin{cases} \frac{\partial u}{\partial t} = \Delta u & \text{in } D \times [0, T], \\ u = f_\ell & \text{on } \Gamma_\ell \times [0, T], \ell = 1, 2, \\ u(\cdot, 0) = 0 & \text{in } D, \end{cases} \quad (1)$$

where f_ℓ , $\ell = 1, 2$ are given smooth functions that satisfy the compatibility conditions $f_\ell(\cdot, 0) = 0$ and $T > 0$ is the final time. The problem (1) is well-posed, for details in the case of classical or weak solutions we refer to [13] or [18, 19], respectively.

Assuming that $f_1 = 0$ and $f_2 \neq 0$, the inverse problem consists in determining the interior boundary curve (or surface in the case of $d = 3$) Γ_1 from the additional knowledge of the heat flux

$$\frac{\partial u}{\partial \boldsymbol{\nu}} = g_2 \quad \text{on } \Gamma_2 \times [0, T], \quad (2)$$

where g_2 is the given smooth function and $\boldsymbol{\nu}$ is the outward unit normal to the boundary $\Gamma = \Gamma_1 \cup \Gamma_2$ of D . The inverse problem (1)-(2) is a nonlinear ill-posed problem. The unique identification of the unknown boundary Γ_1 from the Cauchy data on the Γ_2 is well-known, see [10].

Theorem 1.1. *Let D and \tilde{D} be two double-connected domains with a common exterior boundary Γ_2 and interior boundaries Γ_1 and $\tilde{\Gamma}_1$, respectively. Denote by u and \tilde{u} classical solutions of the initial boundary value problem (1) in the domains D and \tilde{D} , respectively, for $f_1 = 0$ and $f_2 \neq 0$. Assume that $\frac{\partial u}{\partial \boldsymbol{\nu}} = \frac{\partial \tilde{u}}{\partial \boldsymbol{\nu}}$ on $\Gamma_2 \times [0, T]$. Then $\Gamma_1 = \tilde{\Gamma}_1$.*

The article is structured as follows. In section 2 we describe the two-step numerical method for solving the direct problem (1). The application of Newton's method to the inverse problem (1)-(2) along with the final iterative procedure and main steps of the algorithm are given in section 3. The results of numerical experiments of the proposed approach for both two- and three-dimensional domains for exact and noisy Cauchy data are presented in section 4.

2. Numerical solution of the forward problem. In this section we consider the numerical solution of the initial boundary value problem (1), when both boundaries Γ_ℓ , $\ell = 1, 2$ are known. The numerical algorithm based on fundamental sequences method has already been proposed in [3], but with time discretization using the Laguerre transform or Houbolt's method. Here we recall the main steps and use Rothe's method for time discretization instead.

2.1. Time discretization. Following [8], we reduce (1) to the sequence of stationary problems. The time derivative in (1) is approximated by the finite difference approximation on an equidistant mesh

$$t_n = (n+1)h, \quad h = \frac{T}{N+1}, \quad n = -1, 0, \dots, N, \quad N \in \mathbb{N}. \quad (3)$$

We approximate the solution u by the sequence

$$u_n \approx u(\cdot, t_n), \quad n = -1, \dots, N. \quad (4)$$

Then the elements u_n satisfy the sequence of Dirichlet problems for the modified Helmholtz equation with the inhomogeneous right-hand side

$$\begin{cases} \Delta u_n - \mu^2 u_n = \sum_{m=0}^{n-1} \beta_{n-m} u_m & \text{in } D, \\ u_n = f_{\ell,n} & \text{on } \Gamma_\ell, \ell = 1, 2, \end{cases} \quad (5)$$

where $f_{\ell,n} = f_\ell(t_n)$, $\ell = 1, 2$, $n = 0, \dots, N$, $\beta_n = (-1)^n \frac{4}{h}$, $n = 1, \dots, N$, $\mu^2 = \frac{2}{h}$ and $u_{-1} = 0$. In [8], it is shown that the proposed scheme has a second-order approximation in time.

2.2. Fundamental sequence. The sequence of stationary problems (5) is numerically solved by the fundamental sequences method, for this we need to define the fundamental sequence.

Definition 2.1. The sequence of functions Φ_n , for $n = 0, \dots, N$ is the fundamental sequence for the governing equations in (5) provided that

$$\Delta_{\mathbf{x}} \Phi_n(\mathbf{x}, \mathbf{y}) - \mu^2 \Phi_n(\mathbf{x}, \mathbf{y}) - \sum_{m=0}^{n-1} \beta_{n-m} \Phi_m(\mathbf{x}, \mathbf{y}) = \delta(\mathbf{x} - \mathbf{y}),$$

where δ is the Dirac delta function.

The explicit expression for the elements of the fundamental sequence is known, see [8], for $d = 2$ or [9] for $d = 3$ and we recall the result.

Theorem 2.2. The functions Φ_n , $n = 0, \dots, N$ with

$$\Phi_n(\mathbf{x}, \mathbf{y}) = K_0(\mu|\mathbf{x} - \mathbf{y}|)v_n(|\mathbf{x} - \mathbf{y}|) + K_1(\mu|\mathbf{x} - \mathbf{y}|)w_n(|\mathbf{x} - \mathbf{y}|), \quad (6)$$

is the fundamental sequence of the elliptic equations (5) in the sense of Definition 2.1 in the case of two-dimensional domains.

The elements K_0 and K_1 are modified Bessel functions, see [1]. The polynomials v_n and w_n , for $n = 0, \dots, N$ are given by

$$v_n(\rho) = \sum_{m=0}^{\lfloor \frac{n}{2} \rfloor} a_{n,2m} \rho^{2m}, \quad v_0(\rho) = 1 \quad \text{and} \quad w_n(\rho) = \sum_{m=0}^{\lfloor \frac{n-1}{2} \rfloor} a_{n,2m+1} \rho^{2m+1}, \quad w_0(\rho) = 0,$$

with $[p]$ the largest integer not greater than p , for $p \in \mathbb{N}$. The coefficients $a_{n,m}$ for $n = 0, \dots, N$, $m = 0, \dots, n$ are obtained from recurrence relations

$$\begin{aligned} a_{n,0} &= 1; \\ a_{n,n} &= -\frac{1}{2\mu n} \beta_1 a_{n-1,n-1}; \\ a_{n,k} &= \frac{1}{2\mu k} \left\{ 4 \left[\frac{k+1}{2} \right]^2 a_{n,k+1} - \sum_{m=k-1}^{n-1} \beta_{n-m} a_{m,k-1} \right\}, \quad k = n-1, \dots, 1. \end{aligned}$$

Theorem 2.3. *The functions Φ_n , $n = 0, \dots, N$ with*

$$\Phi_n(\mathbf{x}, \mathbf{y}) = \frac{e^{-\mu|\mathbf{x}-\mathbf{y}|}}{|\mathbf{x}-\mathbf{y}|} \tilde{v}_n(|\mathbf{x}-\mathbf{y}|), \quad \mathbf{x} \neq \mathbf{y} \quad (7)$$

is the fundamental sequence of the elliptic equations (5) in the sense of Definition 2.1 in the case of three-dimensional domains.

The polynomials \tilde{v}_n , for $n = 0, \dots, N$, are given by

$$\tilde{v}_n(\rho) = \sum_{m=0}^n \tilde{a}_{n,m} \rho^m,$$

where the coefficients $\tilde{a}_{n,m}$ for $n = 0, 1, \dots$, $m = 0, 1, \dots, n$ are obtained from recurrence relations

$$\begin{aligned} \tilde{a}_{n,0} &= 1; \\ \tilde{a}_{n,n} &= -\frac{1}{2\mu n} \beta_1 \tilde{a}_{n-1,n-1}; \\ \tilde{a}_{n,k} &= \frac{1}{2\mu k} \left\{ k(k+1) \tilde{a}_{n,k+1} - \sum_{m=k-1}^{n-1} \beta_{n-m} \tilde{a}_{m,k-1} \right\}, \quad k = n-1, \dots, 1. \end{aligned}$$

2.3. The application of the fundamental sequence method. Having determined the fundamental sequence by (6) or by (7), we can apply the fundamental sequence method. Following [4], the functions u_n , $n = 0, \dots, N$ are approximated by linear combinations of elements from the fundamental sequence

$$u_n(\mathbf{x}) \approx u_{n,M}(\mathbf{x}) = \sum_{m=0}^n \sum_{j=1}^M \alpha_{m,j} \Phi_{n-m}(\mathbf{x}, \mathbf{y}_j), \quad \mathbf{x} \in D, \quad (8)$$

where $\mathbf{y}_j \notin \bar{D}$, $j = 1, \dots, M$ are selected source points and $\alpha_{m,j}$, $m = 0, \dots, n$, $j = 1, \dots, M$ are coefficients to be determined, for $M \in \mathbb{N}$. The approximate solutions (8) are well defined for all $\mathbf{x} \in \bar{D}$, since the source points are placed outside the domain D , and by direct differentiation can be verified that $u_{n,M}$ satisfy equations (5). Note, that in expressions (8) the coefficients $\alpha_{m,j}$, $m = 0, \dots, n-1$, $j = 1, \dots, M$ have been used for previous elements from the sequence $u_{0,M}, \dots, u_{n-1,M}$, so only the coefficients in front of Φ_0 $\alpha_{n,j}$, $j = 1, \dots, M$ appear for the first time. Thus, we can recursively find the coefficients by collocating on the boundary of the

domain D using a set of collocation points. As a result, we obtain the following recursive systems for determining the coefficients $\alpha_{n,j}$, for $n = 0, \dots, N$:

$$\sum_{j=1}^M \alpha_{n,j} \Phi_0(\mathbf{x}_{\ell,i}, \mathbf{y}_j) = f_{\ell,n}(\mathbf{x}_{\ell,i}) - \sum_{m=0}^{n-1} \sum_{j=1}^M \alpha_{m,j} \Phi_{n-m}(\mathbf{x}_{\ell,i}, \mathbf{y}_j), \quad \ell = 1, 2, \quad (9)$$

where $\mathbf{x}_{\ell,i}$, $\ell = 1, 2$, $i = 1, \dots, \tilde{M}$ are selected collocation points and $\tilde{M} \in \mathbb{N}$ is a number of collocation points on boundaries Γ_ℓ . The obtained linear systems can be written in the matrix form

$$\begin{pmatrix} \Phi_1 \\ \Phi_2 \end{pmatrix} \alpha_n = \begin{pmatrix} \mathbf{f}_{1,n} \\ \mathbf{f}_{2,n} \end{pmatrix}, \quad n = 0, \dots, N, \quad (10)$$

where $\tilde{M} \times M$ sub-matrices Φ_ℓ , $\ell = 1, 2$ are defined as

$$(\Phi_\ell)_{i,j} = \Phi_0(\mathbf{x}_{\ell,i}, \mathbf{y}_j), \quad (11)$$

$i = 1, \dots, \tilde{M}$, $j = 1, \dots, M$, $\tilde{M} \times 1$ sub-vectors $\mathbf{f}_{\ell,n}$, $\ell = 1, 2$, $n = 0, \dots, N$ are defined as

$$(\mathbf{f}_{\ell,n})_i = f_{\ell,n}(\mathbf{x}_{\ell,i}) - \sum_{m=0}^{n-1} \sum_{j=1}^M \alpha_{m,j} \Phi_{n-m}(\mathbf{x}_{\ell,i}, \mathbf{y}_j), \quad i = 1, \dots, \tilde{M} \quad (12)$$

and $M \times 1$ vectors α_n , for $n = 0, \dots, N$ with elements $(\alpha_n)_j = \alpha_{n,j}$, $j = 1, \dots, M$ to be determined.

It is desirable that the ratio between the number of collocation and source points is $2\tilde{M} \geq M$. When the systems (10) are overdetermined (for $2\tilde{M} > M$) they can be solved by the least-squares method. The systems (10) have the same $2\tilde{M} \times M$ matrix and only $2\tilde{M} \times 1$ right-side vectors have to be determined for each $n = 0, \dots, N$, which include already found solutions of previous iterations $\alpha_{m,j}$, for $m < n$, $j = 1, \dots, M$.

2.4. Distributions of the source and collocation points. For the double-connected domain D , the source points have to be placed, according to [2], in the unbounded exterior region of D and in the bounded region enclosed by Γ_1 . We generate an artificial boundary in each of these two regions, and place evenly distributed source points on these boundaries. The collocation points are evenly distributed on the boundaries Γ_ℓ , $\ell = 1, 2$. Let's consider distributions of the source and collocation points for two- and three-dimensional cases separately.

For two-dimensional case, we assume that boundary curves are starlike curves with respect to origin and have following parametrization

$$\Gamma_\ell = \{\gamma_\ell(s) = (\gamma_{\ell,1}(s), \gamma_{\ell,2}(s)), s \in [0, 2\pi]\}, \quad \ell = 1, 2. \quad (13)$$

Then the source points are evenly distributed on the artificial curves by the following rule

$$\mathbf{y}_j = \begin{cases} \eta_2 \gamma_2(s_j), & s_j = \frac{4\pi}{M} j, & j = 1, \dots, \frac{M}{2}, \\ \eta_1 \gamma_1(\tilde{s}_j), & \tilde{s}_j = \frac{4\pi}{M} \left(j - \frac{M}{2}\right), & j = \frac{M}{2} + 1, \dots, M, \end{cases} \quad (14)$$

here we assume that M is an even integer, and $\eta_2 > 1$, $0 < \eta_1 < 1$ are selected parameters. It is known [2] that the source points should be located not too close and not too far from the boundary of the domain. By placing a small number of points away from the boundary, we can get a good approximation accuracy, however, as the distance from the boundary increases, the ill-conditioning of the matrix increases.

On the other hand, the closer the source points are to the boundary, the smaller the matrix condition number will be, but the accuracy of the approximation is worse, and to obtain a good approximation, a larger number of source points must be taken, which, leads to an increase in the computational time. In this work, we choose the following parameters $\eta_2 = 2$ and $\eta_1 = 0.5$.

Collocation points are placed on the boundary curves by the following rule

$$\mathbf{x}_{\ell,i} = \gamma_\ell(s_i), \quad s_i = \frac{2\pi}{\tilde{M}}, \quad i = 1, \dots, \tilde{M}, \quad \ell = 1, 2. \quad (15)$$

For three-dimensional case, we assume that boundary surfaces are star-shaped surfaces with respect to origin and have following parametrization

$$\Gamma_\ell = \{\gamma_\ell(\theta, \phi) = (\gamma_{\ell,1}(\theta, \phi), \gamma_{\ell,2}(\theta, \phi), \gamma_{\ell,3}(\theta, \phi)), \quad \theta \in [0, \pi], \phi \in [0, 2\pi]\}, \quad \ell = 1, 2. \quad (16)$$

The source points are evenly distributed on the artificial surfaces by the following rule

$$\{\mathbf{y}_j\}_{j=1}^M = \{\tilde{\mathbf{y}}_{\ell,j_1,j_2}\}_{\ell=1,j_1=1,j_2=1}^{2,m_1,m_2} : \tilde{\mathbf{y}}_{\ell,j_1,j_2} = \eta_\ell \gamma_\ell(\theta_{j_1}, \phi_{j_2}), \quad (17)$$

with $\theta_{j_1} = \frac{\pi}{m_1+1}j_1$, $\phi_{j_2} = \frac{2\pi}{m_2}j_2$, for $j_1 = 1, \dots, m_1$, $j_2 = 1, \dots, m_2$, $\ell = 1, 2$ and $M = 2m_1m_2$, for some $m_1, m_2 \in \mathbb{N}$. Parameters η_ℓ , $\ell = 1, 2$ are chosen as in two-dimensional case.

Collocation points are evenly distributed on the boundary surfaces Γ_ℓ , $\ell = 1, 2$ by the following rule

$$\{\mathbf{x}_{\ell,i}\}_{\ell=1,i=1}^{2,\tilde{M}} = \{\tilde{\mathbf{x}}_{\ell,i_1,i_2}\}_{\ell=1,i_1=1,i_2=1}^{2,\tilde{m}_1,\tilde{m}_2} : \tilde{\mathbf{x}}_{\ell,i_1,i_2} = \gamma_\ell(\theta_{i_1}, \phi_{i_2}), \quad (18)$$

with $\theta_{i_1} = \frac{\pi}{\tilde{m}_1+1}i_1$, $\phi_{i_2} = \frac{2\pi}{\tilde{m}_2}i_2$, for $i_1 = 1, \dots, \tilde{m}_1$, $i_2 = 1, \dots, \tilde{m}_2$, $\ell = 1, 2$ and $\tilde{M} = \tilde{m}_1\tilde{m}_2$, for some $\tilde{m}_1, \tilde{m}_2 \in \mathbb{N}$.

2.5. Final approximation. Having found solutions of (10), and taking into account (8), we can build the numerical approximation of the solution of the initial boundary value problem for the heat equation (1) at the mesh points t_n , $n = 0, \dots, N$ (3) by

$$u(\mathbf{x}, t_n) \approx u_{n,M}(\mathbf{x}), \quad \mathbf{x} \in D.$$

For the iterative algorithm for the inverse problem, we also need the approximation of the normal derivative of the solution on boundaries Γ_ℓ , $\ell = 1, 2$. From (8), for $n = 0, \dots, N$ we have

$$\frac{\partial u}{\partial \nu}(\mathbf{x}, t_n) \approx \sum_{m=0}^n \sum_{j=1}^M \alpha_{m,j} \Psi_{n-m}(\mathbf{x}, \mathbf{y}_j), \quad \mathbf{x} \in \Gamma_\ell, \quad \ell = 1, 2, \quad (19)$$

where $\Psi_n(\mathbf{x}, \mathbf{y}) = \frac{\partial \Phi_n}{\partial \nu(\mathbf{x})}(\mathbf{x}, \mathbf{y})$, $\mathbf{x} \neq \mathbf{y}$, $\mathbf{x}, \mathbf{y} \in \mathbb{R}^d$, which can be computed via the direct differentiation of functions from the fundamental sequence (for the explicit expressions, we refer to [4, 9]).

The density of the approximations (8) is established, see [4], and can be summarized in the following theorem.

Theorem 2.4. *Let \mathbf{y}_j , $j = 1, \dots, M$ be a set of source points generated by (14) or (17). Then $\Phi_n(\cdot, \mathbf{y}_j)$, $n = 0, \dots, N$, $j = 1, \dots, M$ is a linearly independent and dense set in $L_2(\Gamma)^{N+1}$, and the same holds for the normal derivative of the elements*

in the set. In the case when the dimension $d = 2$ then additionally the transfinite diameter of D should not equal 1.

3. Numerical solution of the inverse problem. We recall, that the main inverse problem is to recover the boundary Γ_1 from the measured heat flux g_2 on the boundary Γ_2 (2) of the solution (1), for $f_1 = 0$ and $f_2 \neq 0$. Let's define a nonlinear operator \mathcal{A} by $\mathcal{A}(\Gamma_1) = \frac{\partial u}{\partial \nu} \Big|_{\Gamma_2 \times [0, T]}$, where u is a solution of the problem (1) corresponding to Γ_1 . Then the inverse problem consists in solving the nonlinear operator equation

$$\mathcal{A}(\Gamma_1) = g_2, \quad (20)$$

for the unknown interior boundary Γ_1 . To solve (20) we apply Newton's method, for this we need to define the domain derivative.

Definition 3.1. For sufficiently small $\epsilon > 0$, fixed $\zeta \in C^2(\Gamma_1, \mathbb{R}^d)$, $d = 2, 3$ and $\Gamma_1^\epsilon = \{\mathbf{x} + \epsilon\zeta(\mathbf{x}), \mathbf{x} \in \Gamma_1\}$, the domain derivative of \mathcal{A} at Γ_1 in the direction ζ is defined by

$$\mathcal{A}'(\Gamma_1; \zeta) = \lim_{\epsilon \rightarrow 0} \frac{1}{\epsilon} [\mathcal{A}(\Gamma_1^\epsilon) - \mathcal{A}(\Gamma_1)].$$

In [10], the existence and explicit representation of the domain derivative is established. The result is summarized in the following theorem.

Theorem 3.2. Let $\zeta \in C^2(\Gamma_1, \mathbb{R}^d)$, $d = 2, 3$ and u is the solution of the initial boundary value problem (1), then

$$\mathcal{A}'(\Gamma_1; \zeta) = \frac{\partial u'}{\partial \nu} \Big|_{\Gamma_2 \times [0, T]}, \quad (21)$$

where u' is a solution of the following initial boundary value problem for the heat equation

$$\begin{cases} \frac{\partial u'}{\partial t} = \Delta u' & \text{in } D \times [0, T], \\ u' = 0 & \text{on } \Gamma_2 \times [0, T], \\ u' = -(\zeta, \nu) \frac{\partial u}{\partial \nu} & \text{on } \Gamma_1 \times [0, T], \\ u(\cdot, 0) = 0 & \text{in } D. \end{cases} \quad (22)$$

For the nonlinear equation (20), we consider the linearized equation

$$\mathcal{A}(\Gamma_1) + \mathcal{A}'(\Gamma_1; \zeta) = g_2. \quad (23)$$

As assumed in (13), for $d = 2$ the Γ_1 is the starlike curve with respect to origin, so it can be represented in the following form

$$\Gamma_1 = \{\gamma_r(s) = r(s)\omega(s), s \in [0, 2\pi]\}, \quad (24)$$

with $\omega(s) = (\cos s, \sin s)$ and $r(s) > 0$ is the unknown radial function.

For $d = 3$, the surface Γ_1 has the star-shaped representation with respect to origin

$$\Gamma_1 = \{\gamma_r(\theta, \phi) = r(\theta, \phi)\omega(\theta, \phi), \theta \in [0, \pi], \phi \in [0, 2\pi]\}, \quad (25)$$

with $\omega(\theta, \phi) = (\sin \theta \cos \phi, \sin \theta \sin \phi, \cos \theta)$ and the unknown radial function $r(\theta, \phi) > 0$.

The linearized equation (23) can be written in the parametric form

$$\mathcal{A}(r) + \mathcal{A}'(r; q) = g_2. \quad (26)$$

The linearized parametric equation has the unique solution, see [10]. It should be solved for q to improve the approximate interior boundary curve (or surface for $d = 3$) Γ_1 , given by the function r via (24) (or (25), for $d = 3$) $r := r + q$, using the current approximation of the function r . By making this procedure iterative, we obtain the standard Newton's method.

The function q is approximated by elements from the finite-dimensional subspace. In two-dimensional domains, we use the trigonometric polynomials of degree less than or equal to \tilde{K} :

$$q(s) \approx \sum_{k=0}^{\tilde{K}} b_k \cos(ks) + \sum_{k=1}^{\tilde{K}} b_{k+\tilde{K}} \sin(ks), \quad s \in [0, 2\pi],$$

where $b_k \in \mathbb{R}$, $k = 0, \dots, 2\tilde{K}$ coefficients to be determined, $\tilde{K} \in \mathbb{N}$. In three-dimensional domains, we use the subspace of real-valued spherical harmonics of degree less than or equal to \hat{K} :

$$q(\theta, \phi) \approx \sum_{k'=0}^{\hat{K}} \sum_{l'=-k'}^{k'} \hat{b}_{k',l'} Y_{k',l'}^R(\theta, \phi), \quad \theta \in [0, \pi], \phi \in [0, 2\pi],$$

where $\hat{b}_{k',l'} \in \mathbb{R}$, $k' = 0, \dots, \hat{K}$, $l' = -k', \dots, k'$ are unknown coefficients, $\hat{K} \in \mathbb{N}$ and real-valued spherical harmonics have the following representation:

$$Y_{k',l'}^R(\theta, \phi) = c_{k',l'}^{l'} P_{k'}^{|l'|}(\cos \theta) \begin{cases} \cos(|l'|\phi), & l' < 0, \\ 1, & l' = 0, \\ \sin(|l'|\phi), & l' > 0, \end{cases}$$

where coefficients are $c_{k',l'}^{l'} = (-1)^{\frac{|l'|-l'}{2}} \sqrt{\frac{2k'+1}{4\pi} \frac{(k'-|l'|)!}{(k'+|l'|)!}}$, $P_{k'}^{|l'|}$ are the associated Legendre functions of degree k' and order $|l'|$, see [1].

For both dimensions the approximation of q can be written in the same form

$$q \approx \sum_{k=0}^K b_k q_k, \quad (27)$$

where $b_k \in \mathbb{R}$ are unknown coefficients and for $d = 2$ the basis functions q_k are:

$$q_k(s) = \begin{cases} \cos(ks), & k = 0, \dots, \tilde{K}, \\ \sin((k - \tilde{K})s), & k = \tilde{K} + 1, \dots, 2\tilde{K}, \end{cases}$$

with $K = 2\tilde{K}$, $s \in [0, 2\pi]$. The functions q_k , for $d = 3$ are:

$$q_k(\theta, \phi) = Y_{k',l'}^R(\theta, \phi), \quad k' = \lceil \sqrt{k} \rceil, \quad l' = k - (k')^2 - k', \quad \text{for } k = 0, \dots, K,$$

with $K = (\hat{K} + 1)^2$, $\theta \in [0, \pi]$, $\phi \in [0, 2\pi]$.

After approximating q by (27) and applying the collocation method to (26), we obtain a linear system for finding the unknown coefficients b_k , $k = 0, \dots, K$:

$$\sum_{k=0}^K b_k \mathcal{A}'(r; q_k)(\hat{\mathbf{x}}_{2,i}, t_n) = g_2(\hat{\mathbf{x}}_{2,i}, t_n) - \mathcal{A}(r)(\hat{\mathbf{x}}_{2,i}, t_n), \quad (28)$$

for $i = 1, \dots, \hat{M}$, $n = 0, \dots, N$, where $\hat{\mathbf{x}}_{2,i} \in \Gamma_2$, $i = 1, \dots, \hat{M}$ are selected collocation points, generated as in rules (15) or (18), but for the number $\hat{M} \in \mathbb{N}$. Clearly, that the obtained linear system is ill-conditioned, therefore, to obtain a stable solution, we apply the Tikhonov regularization method. The system (28) can be written in the matrix form

$$\mathbf{A}\mathbf{b} = (\mathbf{A}_0 \dots \mathbf{A}_K)\mathbf{b} = \mathbf{g}. \quad (29)$$

The $\hat{M}N \times 1$ sub-matrices \mathbf{A}_k , $k = 0, \dots, K$ are defined as

$$(\mathbf{A}_k)_{i+n\hat{M}} = \frac{\partial u'}{\partial \nu}(\hat{\mathbf{x}}_{2,i}, t_n), \quad i = 1, \dots, \hat{M}, \quad n = 0, \dots, N, \quad (30)$$

where u' is a numerical solution of the problem (22), for $u' = -(q_k \boldsymbol{\omega}, \boldsymbol{\nu}) \frac{\partial u}{\partial \nu}$ on Γ_1 , u is a numerical solution of the problem (1), for the current radial function r . The $\hat{M}N \times 1$ vector \mathbf{g} is defined as

$$(\mathbf{g})_{i+n\hat{M}} = g_2(\hat{\mathbf{x}}_{2,i}, t_n) - \frac{\partial u}{\partial \nu}(\hat{\mathbf{x}}_{2,i}, t_n), \quad i = 1, \dots, \hat{M}, \quad n = 0, \dots, N. \quad (31)$$

The $(K+1) \times 1$ vector \mathbf{b} , with $(\mathbf{b})_k = b_k$, $k = 0, \dots, K$ to be determined.

The stable solution of the linear system (29) is a solution of the regularized system

$$(\mathbf{A}^\top \mathbf{A} + \lambda \mathbf{I})\mathbf{b} = \mathbf{A}^\top \mathbf{g}, \quad (32)$$

where $\lambda > 0$ is a given regularization parameter and \mathbf{I} is a $K \times K$ identity matrix.

3.1. The main steps of the iterative algorithm. Let's summarize the main steps of the proposed iterative scheme for the numerical solution of the inverse problem (1)-(2).

- Choose the initial guess of the radial function r . Approximate the boundary Γ_1 according to (24) or (25), for the chosen r .
- Iterative procedure:
 - Evaluate the value of $\mathcal{A}(r)$: solve the forward problem (1) for boundary functions $f_1 = 0$ and given f_2 , by the method described in section 2, using the obtained by (19) heat flux $\frac{\partial u}{\partial \nu}$ at the collocation points $\hat{\mathbf{x}}_{2,1}, \dots, \hat{\mathbf{x}}_{2,\hat{M}}$, compute the vector \mathbf{g} by (31); separately calculate the heat flux at the collocation points $\mathbf{x}_{1,1}, \dots, \mathbf{x}_{1,\hat{M}}$ for the next step.
 - For $k = 0, \dots, K$, compute the sub-matrices \mathbf{A}_k (30), i.e, evaluate the values of the operators $\mathcal{A}'(r; q_k)$ at the collocation points $\hat{\mathbf{x}}_{2,1}, \dots, \hat{\mathbf{x}}_{2,\hat{M}}$, solving forward problems (1) for $u' = -(q_k \boldsymbol{\omega}, \boldsymbol{\nu}) \frac{\partial u}{\partial \nu}$ on Γ_1 and $u' = 0$ on Γ_2 . In this case, the values of elements from the fundamental sequence in (10) can be calculated only once for all k .
 - Solve the regularized system (32) to find the vector \mathbf{b} .
 - Using the obtained vector of coefficients \mathbf{b} , compute the approximation of q by (27) and update the radial function $r := r + q$. Finally, obtain the new approximation of the Γ_1 using (24) or (25).
- Stop the iterative procedure when $\frac{\|q\|_2}{\|r\|_2} < \epsilon$, for a given tolerance $\epsilon > 0$.

4. Numerical examples. The results of numerical examples for the reconstruction of the inner boundary for different domain configurations for two- and three-dimensional domains are presented in this section. In all examples, we generate synthetic data for given functions $f_2 \neq 0$ and $f_1 = 0$, by solving the forward initial boundary value problem (1), by the method described in the section 2, and compute the heat flux g_2 on the outer boundary Γ_2 using (19). To avoid the inverse crime, we consider a double number of source and collocation points compared to the inverse problem.

We consider both cases, when the given Cauchy data on the boundary Γ_2 has no noise and also when some noise is added. In the case of noisy data, the noise is added to the function g_2 to satisfy the condition

$$\|g_2^\delta - g_2\|_{L_2(\Gamma_2 \times [0, T])} \leq \delta,$$

where g_2^δ is the function with the noise and $\delta > 0$ is the noise level (we present results for $\delta = 5\%$).

To calculate the errors of reconstructed boundary curve Γ_1 , we use the following L_2 relative errors, for $d = 2$

$$E = \left(\frac{\int_0^{2\pi} \{r_{ex}(s) - r_{app}(s)\}^2 ds}{\int_0^{2\pi} r_{ex}^2(s) ds} \right)^{1/2} \quad (33)$$

and for $d = 3$

$$E = \left(\frac{\int_0^{2\pi} \int_0^\pi \{r_{ex}(\theta, \phi) - r_{app}(\theta, \phi)\}^2 d\theta d\phi}{\int_0^{2\pi} \int_0^\pi r_{ex}^2(\theta, \phi) d\theta d\phi} \right)^{1/2}, \quad (34)$$

where r_{ex} is the exact radial function and r_{app} is the reconstructed one. For the numerical calculation of these errors, the trapezoidal quadrature rule is used.

The boundary function f_2 is chosen as

$$f_2(\mathbf{x}, t) = t^2 e^{-4t+2} |\mathbf{x}|, \quad \mathbf{x} \in \Gamma_2, \quad t \in [0, T],$$

where the final time is $T = 2$.

In examples 1 and 2 we show results of numerical experiments in two-dimensional domains, and three-dimensional domains are considered in examples 3 and 4.

4.1. Two-dimensional domains. We consider two examples for the two-dimensional domains and use the same parameters for both examples. The number of time nodes is $N + 1 = 10$, number of source points is $M = 64$, number of collocation points $\tilde{M} = \hat{M} = 64$, number of basis functions $K + 1 = 13$. The regularization parameter is $\lambda = 1e - 10$ for exact data and $\lambda = 1e - 04$ for 5% noisy data. The initial guess is a circle with the radius 0.5. Boundary curves configurations are given in the following examples.

Example 1

The exterior boundary curve Γ_2 is a kite-shaped curve with the following parametrization

$$\Gamma_2 = \{\gamma_2(s) = (\cos s, \sin s - 0.5 \sin^2 s + 0.5), \quad s \in [0, 2\pi]\}$$

and the interior boundary curve Γ_1 (to be reconstructed) is an apple-shaped curve with the parametrization

$$\Gamma_1 = \left\{ \gamma_1(s) = \frac{1 + 0.9 \cos s + 0.1 \sin(2s)}{2 + 1.5 \cos s} (\cos s, \sin s), s \in [0, 2\pi] \right\}.$$

For exact data, the approximate curve was obtained after 5 iterations, and the relative error computed by (33) is $E = 2.10e-02$. In the case of noisy data, the solution was obtained after 4 iterations with the relative error $E = 8.22e-02$. In Fig. 1 exact and reconstructed boundary curves Γ_1 are presented in the case of exact (a) and noisy (b) data.

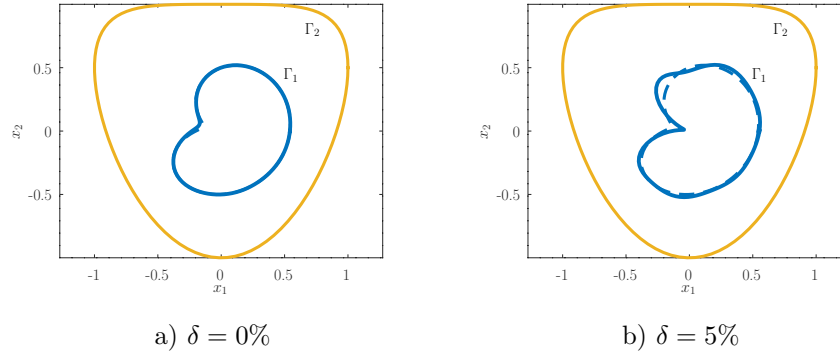


FIGURE 1. Reconstructed (solid line) and exact (dashed line) boundary curves Γ_1 for exact and 5% noisy data for the example 1.

Example 2

The exterior boundary curve Γ_2 is a rounded rectangle with the following parametrization

$$\Gamma_2 = \{ \gamma_2(s) = (\cos^{10} s + \sin^{10} s)^{-0.1} (\cos s, \sin s), s \in [0, 2\pi] \}$$

and the interior boundary curve Γ_1 is a peanut-shaped curve with the parametrization

$$\Gamma_1 = \left\{ \gamma_1(s) = \sqrt{(0.5 \cos s)^2 + (0.25 \sin s)^2} (\cos s, \sin s), s \in [0, 2\pi] \right\}.$$

For exact data, the approximate curve was obtained after 5 iterations, and the relative error computed by (33) is $E = 7.90e-03$. In the case of noisy data, the solution was obtained after 3 iterations with the relative error $E = 9.09e-02$. In Fig. 2 exact and reconstructed boundary curves Γ_1 are presented in the case of exact (a) and noisy (b) data.

4.2. Three-dimensional domains. For both examples, we use the same parameters settings. The number of time nodes is $N + 1 = 10$, number of source points is $M = 256$, number of collocation points $\tilde{M} = \hat{M} = 256$, number of basis functions $K + 1 = 25$. The regularization parameter is $\lambda = 1e-06$ for exact data and $\lambda = 1e-04$ for 5% noisy data. Domain configurations are presented in the following two examples.

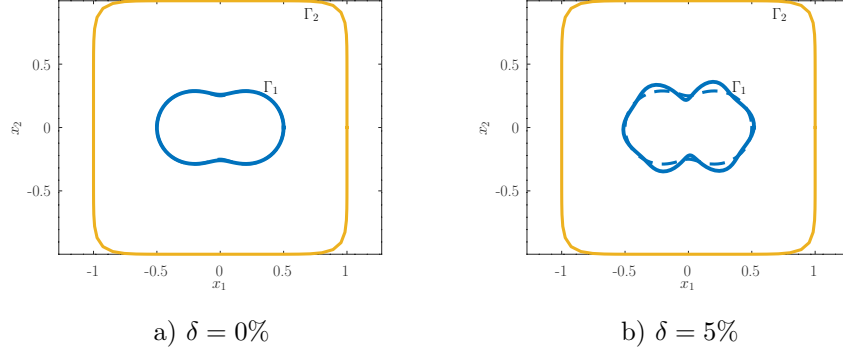


FIGURE 2. Reconstructed (solid line) and exact (dashed line) boundary curves Γ_1 for exact and 5% noisy data for the example 2.

Example 3

The exterior boundary surface Γ_2 is the unit sphere

$$\Gamma_2(\theta, \phi) = \{\gamma_2(\theta, \phi) = (\sin \theta \cos \phi, \sin \theta \sin \phi, \cos \theta), \theta \in [0, \pi], \phi \in [0, 2\pi]\}$$

and the interior boundary surface Γ_1 has the following parametrization

$$\Gamma_1(\theta, \phi) = \{\gamma_1(\theta, \phi) = r_1(\theta, \phi)(\sin \theta \cos \phi, \sin \theta \sin \phi, \cos \theta), \theta \in [0, \pi], \phi \in [0, 2\pi]\},$$

with $r_1(\theta, \phi) = 0.2 \left(0.6 + \sqrt{4.25 + 2 \cos(3\theta)} \right)$. The domain D is presented in Fig. 3a. The initial guess is the sphere with the radius 0.6.

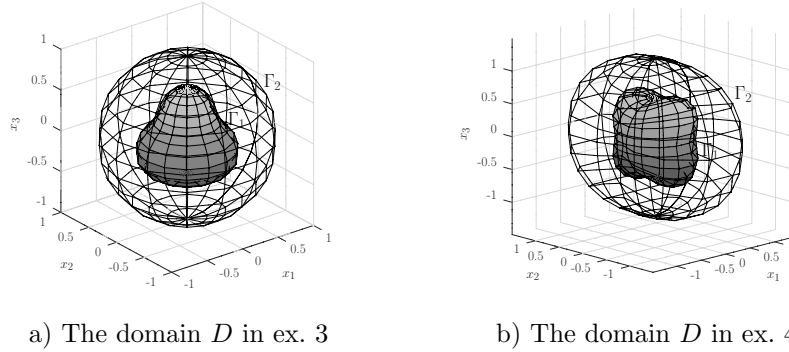


FIGURE 3. Domains used in examples 3 and 4.

For exact data, the approximate surface was obtained after 5 iterations and the relative error computed by (34) is $E = 9.13e - 03$. In the case of noisy data, the solution was obtained after 5 iterations with the relative error $E = 3.42e - 02$. In Fig. 4 exact and reconstructed boundary surfaces Γ_1 are presented in the case of exact (b) and noisy (c) data. To show the error more clearly, we show the sections of the domain and the reconstructed boundary surface at $x_1 = 0$ in Fig. 5.

Example 4

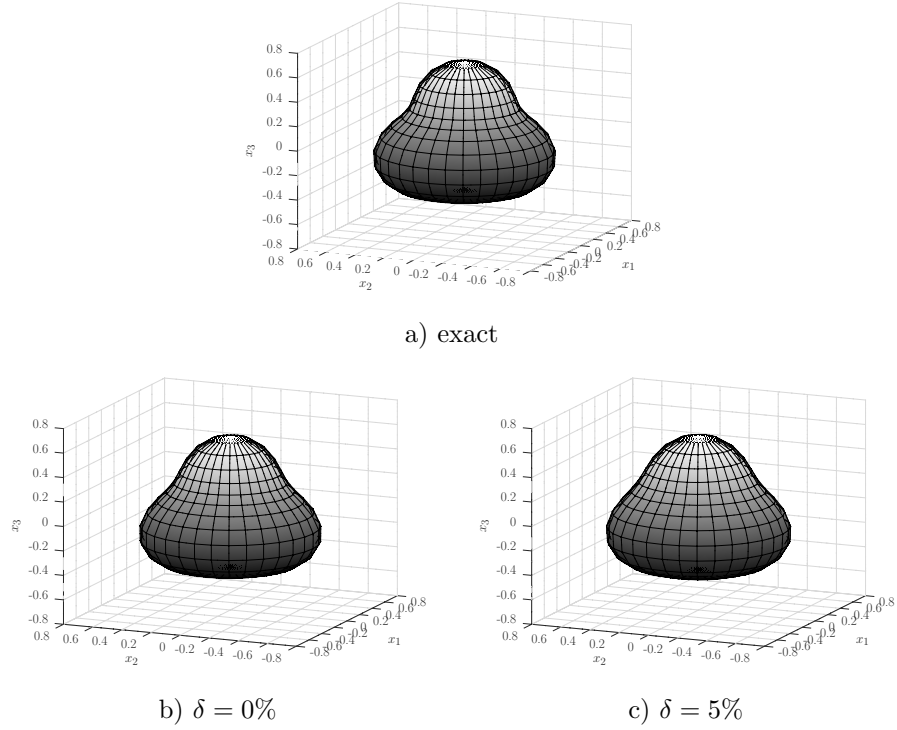


FIGURE 4. Exact (a) and reconstructed boundary surfaces Γ_1 for exact (b) and 5% noisy (c) data for the example 3.

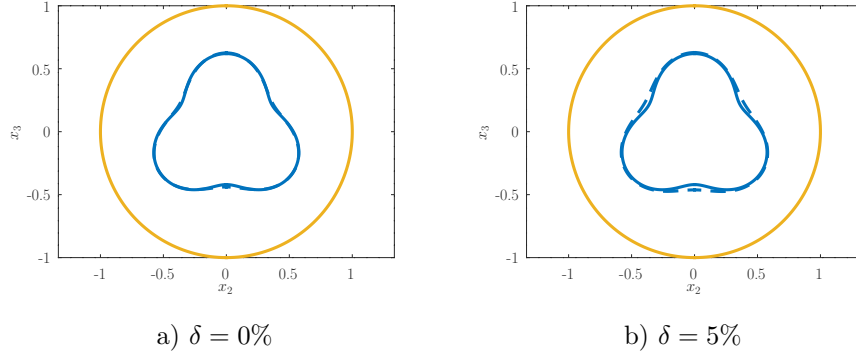


FIGURE 5. Reconstructed (solid blue line) and exact (dashed blue line) sections of boundary surfaces Γ_1 at $x_1 = 0$, for exact and 5% noisy data for the example 3.

The exterior boundary surface Γ_2 has the following parametrization

$$\Gamma_2(\theta, \phi) = \{\gamma_2(\theta, \phi) = r_2(\theta, \phi)(\sin \theta \cos \phi, \sin \theta \sin \phi, \cos \theta), \theta \in [0, \pi], \phi \in [0, 2\pi]\},$$

with $r_2(\theta, \phi) = \sqrt{1.44 + 0.5 \cos(2\phi)(\cos(2\theta) - 1)}$ and the interior boundary surface Γ_1 is a cushion-like surface with the following parametrization

$$\Gamma_1(\theta, \phi) = \{\gamma_1(\theta, \phi) = r_1(\theta, \phi)(\sin \theta \cos \phi, \sin \theta \sin \phi, \cos \theta), \theta \in [0, \pi], \phi \in [0, 2\pi]\},$$

with $r_1(\theta, \phi) = \frac{3}{2} \sqrt{0.8 + 0.2(\cos(2\phi) - 1)(\cos(4\theta) - 1)}$. The domain D is presented in Fig. 3b. The initial guess is a sphere with the radius 0.7.

For exact data, the approximate surface was obtained after 4 iterations and the relative error is $E = 3.54e - 02$. In the case of noisy data, the solution was obtained after 3 iterations with the relative error $E = 6.07e - 02$. In Fig. 6 exact and reconstructed boundary surfaces Γ_1 are presented in the case of exact (b) and noisy (c) data, and the sections of the domain and the reconstructed boundary surface at $x_1 = 0$ are presented in Fig. 7.

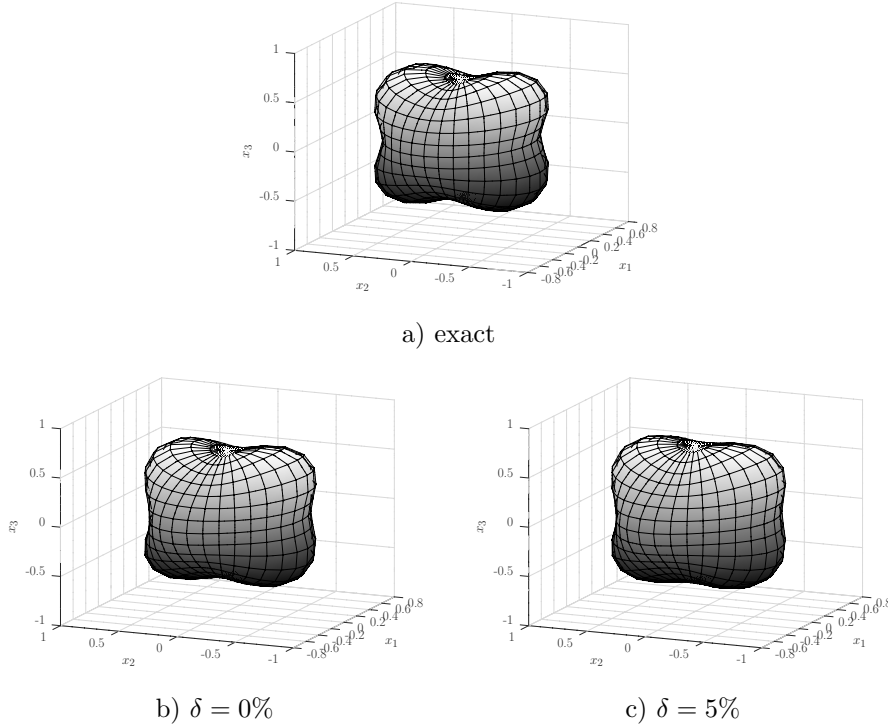


FIGURE 6. Exact (a) and reconstructed boundary surfaces Γ_1 for exact (b) and 5% noisy (c) data for the example 4.

All presented numerical results have been performed in Octave and executed on an ordinary workstation having an Intel(R) Core(TM) i7 CPU at 2.60 GHz. The execution time of the proposed algorithm for the first example ($d = 2$) is near 4 minutes for exact data and 3 minutes for noisy data. For the third example ($d = 3$), the execution time is near 100 minutes for both exact and noisy data.

In all examples we consider only 5% of noise, for more than 10% of noise the results become imprecise. For the initial guess, we assume that a priori information about the location and size of the inner boundary is given, and we focus on

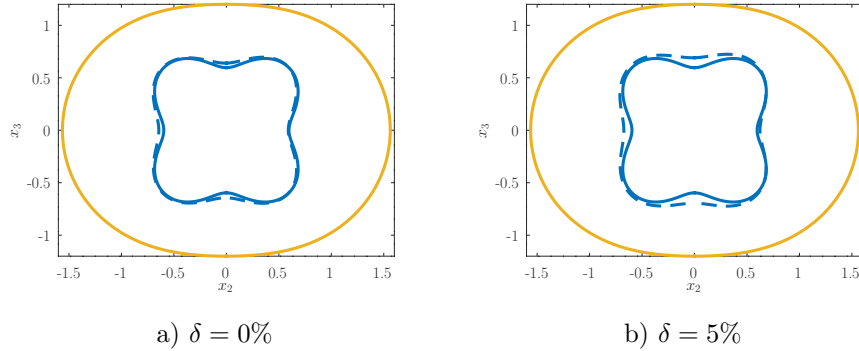


FIGURE 7. Reconstructed (solid blue line) and exact (dashed blue line) sections of boundary surfaces Γ_1 at $x_1 = 0$, for exact and 5% noisy data for the example 4.

the reconstruction; in future research, we will use genetic algorithms as a more sophisticated selection technique.

Conclusions. The nonlinear inverse problem of reconstruction of the inner boundary of the double-connected domain from the overdetermined Cauchy data on the outer boundary of the solution of the heat conduction equation is considered. The problem is numerically solved by the regularized Newton's method, at each step of which the linearized equation is solved to obtain a new update of the approximation of the radial function of the inner boundary. The linearized equation consists of normal derivatives of the solutions of unsteady direct problems. It is numerically solved by the projection method, that is, the solution is approximated by the linear combination of elements from the corresponding finite-dimensional subspace, and the unknown coefficients are found by the collocation method.

The two-step numerical method for solving the linear direct problem is proposed. In the first step, using Rothe's method, the unsteady problem for the heat equation is reduced to the sequence of steady-state problems with the modified inhomogeneous Helmholtz equation. In the second step, the obtained sequence is fully discretized by the fundamental sequences method, that is, the unknown solutions of the stationary sequence are approximated by linear combinations of the elements from the fundamental sequence, and these combinations exactly satisfy equations. The unknown coefficients are found from the Dirichlet boundary conditions using the collocation method.

Numerical results for both two- and three-dimensional domains confirm the effectiveness and applicability of the proposed numerical scheme for exact and noisy data cases.

REFERENCES

- [1] M. Abramowitz and I.A. Stegun, *Handbook of Mathematical Functions with Formulas, Graphs, and Mathematical Tables*, Dover Publications, New York, 1972.
- [2] C. J. S. Alves, [On the choice of source points in the method of fundamental solutions](#), *Eng. Anal. Bound. Elem.*, **33** (2009), 1348-1361.
- [3] I. Borachok, [On the method of fundamental solutions for the time dependent Dirichlet problems](#), *Journal of Numerical and Applied Mathematics*, **3** (2021), 33-44.

- [4] I. Borachok, R. Chapko and B. T. Johansson, [A method of fundamental solutions for heat and wave propagation from lateral Cauchy data](#), *Numer Algor*, **89** (2022), 431-449.
- [5] I. Borachok, R. Chapko and B. T. Johansson, [Numerical solution of a Cauchy problem for Laplace equation in 3-dimensional domains by integral equations](#), *Inverse Problems in Science and Engineering*, **24** (2016), 1550-1568.
- [6] R. Brügger, H. Harbrecht and J. Tausch, [On the numerical solution of a time-dependent shape optimization problem for the heat equation](#), *SIAM Journal on Control and Optimization*, **59** (2021), 931-953.
- [7] R. Chapko, O. Ivanyshyn and O. Protsyuk, [On a nonlinear integral equation approach for the surface reconstruction in semi-infinite-layered domains](#), *Inverse Problems in Science and Engineering*, **21** (2012), 547-561.
- [8] R. Chapko and B. T. Johansson, [A boundary integral equation method for numerical solution of parabolic and hyperbolic Cauchy problems](#), *Appl. Numer. Math.*, **129** (2018), 104-119.
- [9] R. Chapko and B. T. Johansson, [Numerical solution of the Dirichlet initial boundary value problem for the heat equation in exterior 3-dimensional domains using integral equations](#), *J. Eng. Math.*, **103** (2017), 23-37.
- [10] R. Chapko, R. Kress and J. Yoon, [On the numerical solution of an inverse boundary value problem for the heat equation](#), *Inverse Problems*, **14** (1998), 853-867.
- [11] R. Chapko, R. Kress and J. Yoon, [An inverse boundary value problem for the heat equation: the Neuman condition](#), *Inverse Problems*, **15** (1999), 1033-1046.
- [12] G. Fairweather and A. Karageorghis, [The method of fundamental solutions for elliptic boundary value problems](#), *Adv. Comput. Math.*, **9** (1998), 69-95.
- [13] A. Friedman, *Partial Differential Equations of Parabolic Type*, Englewood Cliffs, NJ: Prentice-Hall, 1964.
- [14] H. Harbrecht and J. Tausch, [On the numerical solution of a shape optimization problem for the heat equation](#), *SIAM Journal on Scientific Computing*, **35** (2013), A104-A121.
- [15] O. Ivanyshyn and R. Kress, [Identification of sound-soft 3D obstacles from phaseless data](#), *Inverse Problems and Imaging*, **4** (2010), 131-149.
- [16] A. Karageorghis and D. Lesnic, [Detection of cavities using the method of fundamental solutions](#), *Inverse Probl. Sci. Eng.*, **17** (2009), 803-820.
- [17] V. D. Kupradze and M. A. Aleksidze, [The method of functional equations for the approximate solution of certain boundary value problem](#), *Computational Mathematics and Mathematical Physics*, **4** (1964), 633-725.
- [18] O.A. Ladyzenskaja, V.A. Solonnikov and N.N. Uralceva, *Linear and Quasilinear Equations of Parabolic Type*, Providence, RI: American Mathematical Society, 1968.
- [19] J.L. Lions and E. Magenes, *Non-Homogeneous Boundary Value Problems and Applications: Vol 2*, Berlin: Springer, 1972.
- [20] L. Marin and L. Munteanu, [Boundary reconstruction in two-dimensional steady state anisotropic heat conduction using a regularized meshless method](#), *International Journal of Heat and Mass Transfer*, **53** (2010), 5815-5826.

Received July 2024; revised November 2024; early access November 2024.